Mechanical Properties of Cr-Al-N-O Thin Films Prepared by Pulsed Laser Deposition

Makoto Hirai, Tsuneo Suzuki, Hisayuki Suematsu, Weihua Jiang and Kiyoshi Yatsui
Fax: 81-258-47-9890, e-mail: hirai@etigo.nagaokaut.ac.jp
Extreme Energy-Density Research Institute, Nagaoka University of Technology, Nagaoka, Niigata 940-2188

Chromium aluminum oxynitride (Cr-Al-N-O) thin films have been successfully prepared by pulsed laser deposition. Root mean square rougfness (*RMS*), hardness (*H*) and friction coefficient (μ), which were important parameters to coating material for cutting tools, were evaluated for Cr-N-O and Cr-Al-N-O thin films. As a result, the Cr-N-O thin film had *RMS* = 26.3 nm, *H* = 21.5 GPa and μ = 0.88, whereas the Cr-Al-N-O thin film with aluminum content in cations of 35 at. % had *RMS* = 76.0 nm, *H* = 39.0 GPa and μ = 0.67. Thus, the friction coefficient of the thin films was reduced by enhancement of hardness rather than decrease of surface roughness. In addition, the improvement of friction coefficient was also considered to be the result with that adhesion wear occurs hardly due to dissolved aluminum atoms.
Key words: chromium aluminum oxinitride, hardness, roughness, friction coefficient, wear resistance

1. INTRODUCTION

Titanium aluminum nitride (Ti-Al-N), where had high hardness and oxidation resistance, has been widely used as coating material for cutting tool [1]. However, in recent years, it is required to enhance the wear resistance of the coating material for the protection of environment. To satisfy such requirement, it is necessary to develop new material having the properties superior to Ti-Al-N.

Chromium aluminum nitride (Cr-Al-N) is paid much attention as the replacement of Ti-Al-N, and such thin films have been synthesized by physical vapor deposition (PVD) [2-5]. As a result, it was found that the Cr-Al-N thin films have approximately 100 °C higher oxidation temperature than the Ti-Al-N thin films [1,5]. However, the hardness of Cr-Al-N thin films was observed slightly lower than that of the Ti-Al-N thin films [1,3,4]. By using pulsed laser deposition (PLD), the authors have prepared chromium aluminum oxynitride (Cr-Al-N-O) thin films, which were dissolved oxygen atoms in the Cr-Al-N thin films [6-8]. The Cr-Al-N-O thin films had almost same oxidation temperature as the Cr-Al-N thin films [1,7], and were Vickers hardness (HV) of approximately 1000 harder than the Ti-Al-N thin film when aluminum content in cations (x) was 25 at. % [1,8].

Wear resistance of the coating material was improved by the reduction of friction coefficient other than the enhancement of hardness and oxidation temperature. However, there were no experimental data on the friction coefficient of the Cr-Al-N-O thin films. Thus, this investigation was undertaken to clarify the friction coefficient of the Cr-Al-N-O thin films.

2. EXPERIMENTAL SETUP

Thin films were deposited by the irradiation of a Nd: yttrium aluminum garnet (λ = 355 nm) laser beam onto target. The laser was electro-optically Q switched by Pockels cell to produce intense pulses of short duration (7 ns) by the repetition rate of 10 Hz. The laser beam was concentrated by a lens, and the fluence (*F*) was adjusted to 1 and 5 J/cm² on the target. Plates of chromium nitride (Cr_2N) and aluminum nitride (AlN) were used as the target. Cation composition of the thin films was controlled by changing the irradiated area of Cr_2N (S_{Cr_2N}) and AlN (S_{AlN}) plates. Surface area ratio of targets (S_R) is expressed by the following equation: $S_R = S_{AlN} / (S_{Cr_2N} + S_{AlN})$. The chamber was evacuated to 5×10^{-6} Torr using rotary and cryo pumps. Experiments were carried out under the pressure of 1×10^{-5} Torr. A single-crystal (100)-oriented silicon (Si) substrate was placed at the distance (d_{TS}) of 10 and 40 mm from the target. The substrate temperature was controlled at 400 °C by using a heater and a thermocouple. Typical experimental conditions are listed in Table I.

Table I Experimental conditions

Fluence (*F*)	1, 5 J/cm²
Target	Cr_2N, AlN
Substrate	Si (100)
Distance from target to Substrate (d_{TS})	10, 40 mm
Substrate temperature	400 °C
Pressure	1×10^{-5} Torr
Surface area ratio of target $S_R = S_{AlN} / (S_{Cr_2N} + S_{AlN})$	0-100 %

A Rutherford backscattering spectroscope (NHV NT-1700HS) was applied to measure the composition of the thin films, where were prepared by changing S_R. The crystal structure of the thin films was identified by a X-ray diffractometer (RIGAKU RINT 2500 HF⁺/PC). The diffraction patterns were recorded using a Cu K_α

radiation of 1.5418 Å under the operating conditions of 50 kV and 300 mA. Surface state of the thin films was determined in the area of 10×10 μm with atomic force microscope (SEIKO SPI3800). The measurement was done seven times in each thin film, and root mean square roughness (*RMS*) was evaluated to extract the minimum and maximum values. Hardness (*H*) was measured by using a microhardness tester (FISCHER H-100) equipped by a Vickers diamond indenter. The conditions of indentation tests were as follows: maximum force, 25 mN; indenting rate, 0.83 mN/s; the number of measurement, 7 times; temperature, 25 °C. Friction coefficient (*μ*) was determined with the ablation tester (CSEM TRIBOMETER) of ball-on-disc type. The conditions for the friction coefficient measurement were as follows: ball of 6 mm in diameter; SUJ2 (Fe-1 % C-1.3 % Cr), load; 2 N, rotating speed; 50 mm/s and sliding distance; 100 m.

3. RESULTS AND DISCUSSION

Figure 1 shows a typical spectrum obtained by Rutherford backscattering spectroscopy (RBS) for thin film prepared at $F = 5$ J/cm^2, $d_{TS} = 10$ mm and $S_R = 75$ %. In Fig. 1, dots are experimental results, while the solid line corresponds to the simulated result. In the simulation, the composition of a thin film was calculated from the Rutherford backscattering energy of helium (He) ions that were entered to the thin film. From the result of the simulation, it was found that the composition of the thin film is $Cr_{0.11}Al_{0.39}N_{0.25}O_{0.25}$. This result indicated that the compositions of cations (Cr and Al) and anions (N and O) in the thin film become equal. Chromium, aluminum and nitrogen atoms in the thin film were provided from Cr_2N and AlN targets, whereas oxygen atoms may be incorporated from residual gas in the deposition chamber.
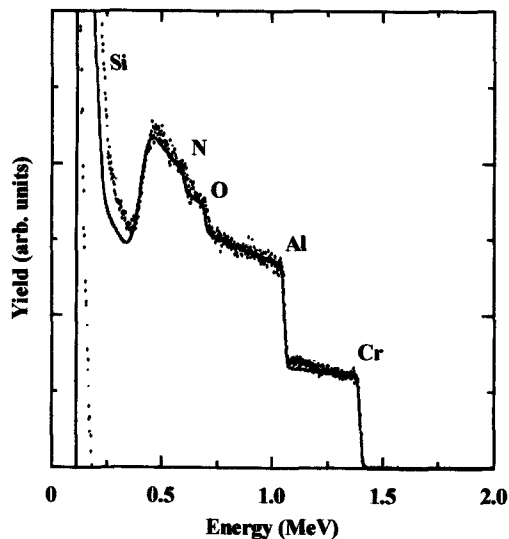
Figure 2 shows cation composition of thin films as a function of surface area ratio of targets. The thin films were prepared by changing S_R from 0 to 100 % under the condition of $F = 1$ J/cm^2 and $d_{TS} = 40$ mm. In Fig. 2, the cation composition of the thin films, which showed the aluminum content in cations, was measured by RBS. In addition, the dotted line indicates the linear dependence of *x* upon S_R. As a result, *x* could be easily controlled by changing S_R, although the measurement result expressed by circles was a little bit larger than the line at $S_R = 25$ %. Although solid solution thin films were prepared by sputtering and ion-plating methods, they were difficult to control composition [2-5]. In contrast, the PLD method could control the composition only by changing S_R.
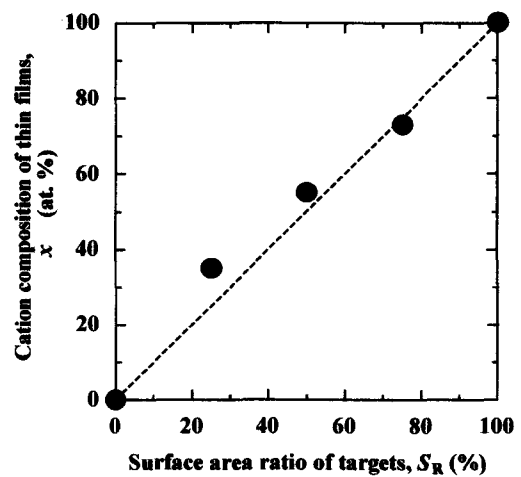
Fig. 2   Cation composition of thin films as a function of surface area ratio of targets.

Fig. 1   A typical spectrum obtained by RBS for thin film prepared at $F = 5$ J/cm^2, $d_{TS} = 10$ mm and $S_R = 75$ %.
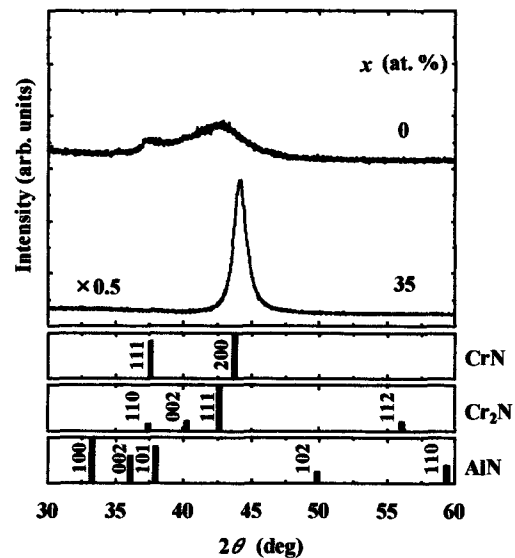
Fig. 3   XRD patterns of thin films with $x = 0$ and 35 at. %.

Figure 3 shows XRD patterns of thin films with x = 0 and 35 at. %. JCPDS card data of chromium nitride (CrN), Cr_2N and AlN was shown under the diffraction results for comparison [9-11]. In Fig. 3, the intensity of diffracted X-ray from the thin film with x = 35 at. % was multiplied by 0.5. Diffraction peaks of the thin film with x = 0 at. % appeared broadly at the positions attributed to Cr_2N. In the thin film with x = 35 at. %, the diffraction peak, where was attributable to CrN (B1 structure) 200, shifted to higher angle. The fact can be explained by the substitution of aluminum atoms for partial chromium ones in B1 phase.
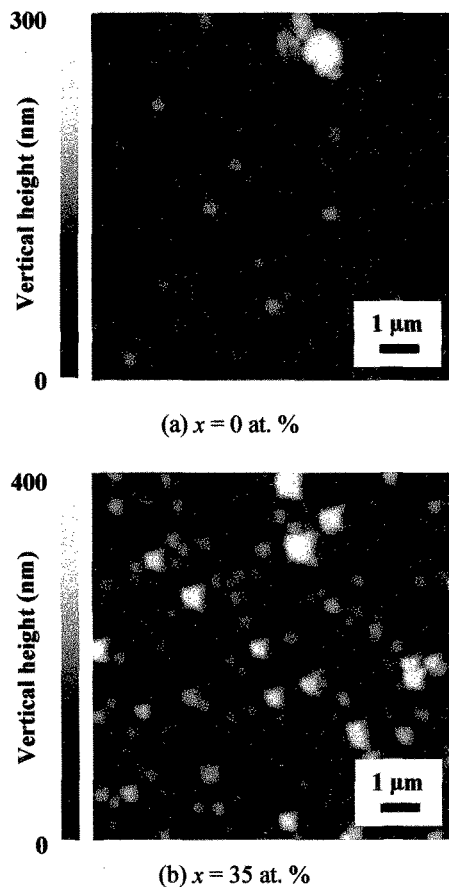

(a) x = 0 at. %

(b) x = 35 at. %

Fig. 4   AFM images of thin films with x = 0 and 35 at. %.

Figure 4 shows atomic force microscopy (AFM) images of thin films with x = 0 and 35 at. %. As can be seen in Fig. 4 (a), there were some spherical particles on the thin film with x = 0 at. %. These particles, which are a common feature of laser-ablated thin films, are called droplets. The diameter of the big droplet was observed to be approximately 1.0 μm. On the other hand, in Fig. 4 (b), the thin film with x = 35 at. %, where was featured by square facets, was found to reflect orientation of Si substrate. This fact was consistent with that the thin film with x = 35 at. % had B1 (cubic) structure with [200] preferred orientation, as shown in Fig. 3. In addition, *RMS* of

the thin films with x = 0 and 35 at. % was 26.3 ± 9.0 and 76.0 ± 7.0 nm, respectively. Thus, a rougher surface of the thin film with x = 35 at. % was revealed to be due to the formation of square facets.

Figure 5 shows loading and unloading curves of thin films with x = 0 and 35 at. %. In Fig. 5, filled circles and triangles showed loading curves, whereas open ones indicated unloading curves. When the maximum load of 25 mN was applied on each thin film, the indentation depth of the thin films with x = 0 and 35 at. % was 0.23 and 0.19 μm, respectively. Thus, the indentation depth was observed to be less than a tenth of the thin film thickness, which was approximately 4 μm. Moreover, the thin film with x = 35 at. % was found to show the lesser amount of plastic strain. This fact indicated that the deformation inhibits due to the substitution of aluminum atoms for partial chromium ones in B1 phase. Hardness is calculated as

$$H = \frac{2F_{L_{max}}}{\alpha d} \quad (1)$$

where $F_{L_{max}}$ is the maximum load, α is the coefficient depending on the geometry of the tip and d is the indentation depth at $F_{L_{max}}$. By using the equation (1), the hardness of the thin films with x = 0 and 35 at. % was found to be 21.5 and 39.0 GPa, respectively.
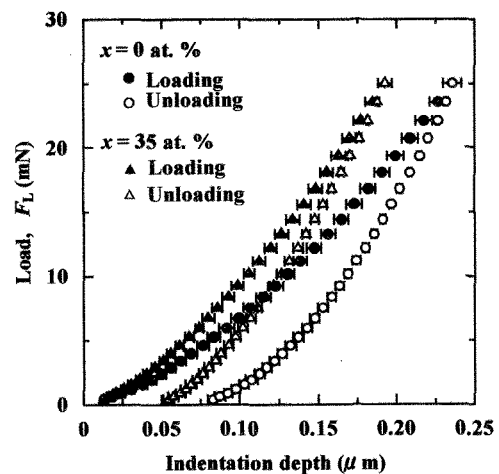

Fig. 5   Loading and unloading curves of thin films with x = 0 and 35 at. %.

Figure 6 shows friction coefficient of thin films with x = 0 and 35 at. % as a function of sliding distance. As a result, friction coefficient of the thin films with x = 0 and 35 at. % was approximately 0.88 and 0.67, respectively. Thus, friction coefficient was clarified to improve by substitution of aluminum atoms. Table II shows properties of thin films with x = 0 and 35 at. %. The thin film with x = 35 at. % was approximately 3 times rougher than the thin film with x = 0 at. %. The fact was a result of that the thin film with x = 35 at. % is formed by larger crystal grains, as shown in Fig. 3 and 4. In addition, the thin films with x = 35 at. % had high hardness of 39 GPa due to solid solution hardening. Friction coefficient of a material

has been known to reduce with smoothing and hardening the material [12-14]. The friction coefficient of the thin film with x = 35 was approximately 0.2 lower than that of the thin film with x = 0 at. %. Thus, hardness was clarified to be more effective for reducing in friction coefficient, compared with surface roughness. In addition, the improvement of friction coefficient was also considered to be the result with that the adhesion between the thin film and SUJ2 ball occurs hardly due to dissolved aluminum atoms.
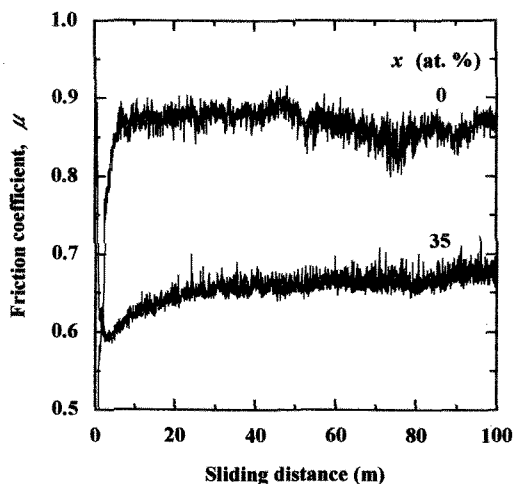

Fig. 6   Friction coefficient of thin films with x = 0 and 35 at. % as a function of sliding distance.

Table II   Properties of thin films with x = 0 and 35 at. %

x (at. %)	RMS (nm)	H (GPa)	μ
0	26.3 ± 9.0	21.5	0.88
35	76.0 ± 7.0	39.0	0.67

4. CONCLUSIONS

From these experimental results, the authors obtained following conclusions:

1) Using the PLD method, Cr-Al-N-O thin film was successfully prepared by changing S_R.

2) Cr-Al-N-O thin film with x = 35 at. %, where had B1 structure with [200] preferred orientation, was rougher and harder than Cr-N-O thin film.

3) A lot of square facets appeared on the surface of the Cr-Al-N-O thin film with x = 35 at. %.

4) Friction coefficient of Cr-Al-N-O thin film with x = 35 at. % was approximately 0.2 lower than that of Cr-N-O thin film.

REFERENCES

[1] T. Ikeda and H. Satoh, *Thin Solid Films*, **195**, 99-110 (1991).

[2] Y. Makino and K. Nogi, *Surf. & Coatings Technol.*, **98**, 1008-1012 (1998).

[3] J. Vetter, E. Lugscheider and S. S. Guerreiro, *Surf. & Coatings Technol.*, **98**, 1233-1239 (1998).

[4] Y. Ide, K. Kishitake and T. Nakamura, *J. Japan Inst. Metals*, **63**, 1576-1583 (1999).

[5] Y. Ide, K. Inada, T. Nakamura and K. Kishitake, *Materia Japan*, [in Japanease] **40**, 815-816 (2001).

[6] M. Hirai, Y. Ueno, T. Suzuki, W. Jiang, C. Grigoriu and K. Yatsui, *Jpn. J. Appl. Phys.*, **40**, 1056-1060 (2001).

[7] M. Hirai, H. Saito, T. Suzuki, H. Suematsu, W. Jiang and K. Yatsui, *Thin Solid Films*, **407**, 122-125 (2002).

[8] M. Hirai, H. Saito, T. Suzuki, H. Suematsu, W. Jiang and K. Yatsui: *Proc. Material Research Society Symposium*, **697**, P7.7.1-6 (Boston, 2002).

[9] Powder Diffraction File, JCPDS International Center for Powder Diffraction Data, Swarthmore, PA: CrN (11-0065).

[10] Powder Diffraction File, JCPDS International Center for Powder Diffraction Data, Swarthmore, PA: Cr₂N (35-0803).

[11] Powder Diffraction File, JCPDS International Center for Powder Diffraction Data, Swarthmore, PA: AlN (25-1133).

[12] M. M. Khruschov: *Proc. Conf. on Lub. and Wear*, p. 655 (London, 1957).

[13] D. C. Reigada and F. L. Freire Jr., *Surf. & Coatings Technol.*, **142-144**, 889-893 (2001).

[14] D. Kim and S. Kim, *Surf. & Coatings Technol.*, **157**, 66-71 (2002).